the source to the interface remains the same in both problems). This half-space pattern is a "lens" type of pattern, which is nearly constant out to the critical angle, and rapidly decaying beyond. This lens type of pattern shows a directivity enhancement relative to the same source in free space, although the directivity is not as large as it is for an optimized lossless slab. Furthermore, the directivity enhancement for the half-space configuration is due solely to a ray-optic effect, and not a leaky wave.

REFERENCES

1. K.C. Gupta, Narrow-beam antennas using an artificial dielectric medium with permittivity less than unity, Electron Lett 7 (1971), 16–18.
2. I.J. Bahl and K.C. Gupta, A leaky-wave antenna using an artificial dielectric medium, IEEE Trans Antennas Propag 22 (1974), 119–122.
3. G. Poilasne, P. Pouliguen, J. Lenormand, K. Mahdjoubi, C. Terret, and P. Gelin, Theoretical study of interactions between antennas and metallic photonic bandgap materials, Microwave Opt Technol Lett 15 (1997), 384–389.
4. S. Enoch, G. Tayeb, P. Sabouroux, N. Guerin, and P. Vincent, A metamaterial for directive emission, Phys Rev Lett 89 (2002), 213902–1–213902–4.
5. G. Lovat, P. Burghignoli, F. Capolino, D.R. Jackson, and D.R. Wilton, Analysis of directive radiation from a line source in a metamaterial slab with low permittivity, IEEE Trans Antennas Propagat 54 (2006), 1017–1030.
6. T. Tamir and A.A. Oliner, The influence of complex waves on the radiation field of a slot-excited plasma layer, IRE Trans Antennas Propag 10 (1962), 55–65.
7. G. Lovat, P. Burghignoli, F. Capolino, and D.R. Jackson, Highly-directive planar leaky-wave antennas: A comparison between metamaterial-based and conventional designs, EuMA (European Microwave Association) Proceedings, in press.
8. J. Brown, Artificial dielectrics having refractive indices less than unity, Proc IEEE 100 (1953), 51–62.
9. W. Rotman, Plasma simulation by artificial dielectrics and parallel-plate media, IRE Trans Antennas Propag 10 (1962), 82–95.
10. J.B. Pendry, A.J. Holden, W.J. Stewart, and I. Youngs, Extremely low frequency plasmons in metallic mesostructures, Phys Rev Lett 76 (1996), 4773–4776.
11. J.B. Pendry, A.J. Holden, D.J. Robbins, and W.J. Stewart, Low frequency plasmons in thin-wire structures, J Phys: Condens Matter 10 (1998), 4785–4809.
12. P.A. Belov, S.A. Tretyakov, and A.J. Viitanen, Dispersion and reflection properties of artificial media formed by regular lattices of ideally conducting wires, J Electromag Waves Appl 16 (2002), 1153–1170.
13. P.A. Belov, R. Marquès, S.I. Maslovski, M. Silveirinha, C.R. Simovski, and S.A. Tretyakov, Strong spatial dispersion in wire media in the very large wavelength limit, Phys Rev B: Solid State 67 (2003), 113103–1–113103–4.
14. L.B. Felsen and N. Marcuvitz, Radiation and scattering of waves, IEEE Press, Piscataway, NJ, 1994.

VERIFICATION OF IMPEDANCE MATCHING AT THE SURFACE OF LEFT-HANDED MATERIALS

Koray Aydin,[1,2] Irfan Bulu,[1,2] and Ekmel Ozbay[1–3]
[1] Nanotechnology Research Center
Bilkent University
Bilkent, Ankara 06800 Turkey
[2] Department of Physics
Bilkent University
Bilkent, Ankara 06800 Turkey
[3] Department of Electrical and Electronics Engineering
Bilkent University
Bilkent, Ankara 06800 Turkey

Received 2 June 2006

ABSTRACT: *Impedance matching at the surface of left-handed materials (LHM) is required for certain applications including a perfect lens. In this study, we present the experimental and theoretical verification of an impedance-matched LHM to free space. Reflection characteristics of both one-dimensional and two-dimensional LHM were investigated. The reflection was observed to be very low at a narrow frequency range. FDTD simulations and retrieval procedures were used to theoretically verify impedance matching. By varying the number of layers along the propagation direction, the ultralow reflection at specific frequencies was shown to be independent of the sample thickness.* © 2006 Wiley Periodicals, Inc. Microwave Opt Technol Lett 48: 2548–2552, 2006; Published online in Wiley InterScience (www.interscience.wiley.com). DOI 10.1002/mop.22003

Key words: *left-handed materials; metamaterials; reflection; impedance matching; perfect lens*

1. INTRODUCTION

Materials that possess a negative index of refraction have become a remarkable research area in recent years because of their interesting properties and novel applications. The intriguing physics of a medium having a negative refractive index was discussed by Veselago theoretically nearly four decades ago [1]. Veselago predicted that a medium with simultaneous negative permittivity along with negative permeability exhibits unusual physical properties; among them are negative refraction, reversal of Doppler shift, and backward Cerenkov radiation. In the pioneering work of Pendry et al., a metallic thin wire grid was shown to exhibit a plasma frequency in the microwave regime, below which the effective permittivity takes negative values [2]. Thereafter, a split-ring resonator (SRR) structure is proposed to have $\mu(\omega) < 0$ near the magnetic resonance frequency [3]. Experimental realization of left-handed metamaterials (LHM) was achieved by arranging $\varepsilon(\omega) < 0$ media and $\mu(\omega) < 0$ media periodically [4, 5]. A left-handed transmission band was observed at the frequencies where both ε and μ are negative. This was later followed by the direct measurement of a negative refractive index by means of different methods [6–8]. Recent experimental and theoretical studies have reported the exotic electromagnetism of LHMs, such as negative phase velocity [7, 9], backward wave radiation [10], and perfect lens behavior [11]. Special interest was given to the perfect lens phenomena where the amplitude of evanescent waves are restored, enabling the so-called subwavelength focusing. Aydin et al. recently reported subwavelength focusing by using a LHM flat lens [12]. Most of the experimental measurements on LHMs are performed on microwave frequency region; but there is a tendency to increase the operation frequency up to terahertz [13, 14] and even optical frequencies [15].

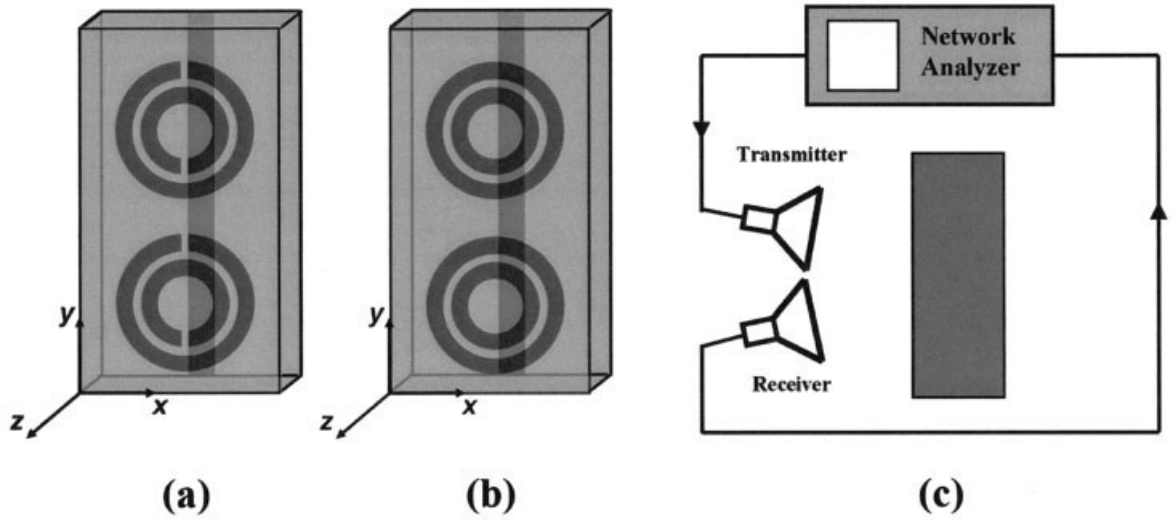

Figure 1 Schematic picture of (a) LHM composed of SRRs and wires and (b) CMM composed of CRRs and wires on a dielectric board. (c) Experimental setup for measuring the reflection from the surface of a LHM

It is possible to define the LHM with effective medium parameters, since the operation wavelength is much greater than the unit size and lattice constant of the constituents. Electromagnetic wave propagation through media with simultaneously negative values of permittivity and permeability were studied extensively in the literature [16–18]. Significant amount of theoretical analyses were made to obtain effective permittivity and permeability values by using various retrieval procedures [19–25]. Parameters are retrieved by using the transmission and reflection coefficients. Although different approaches are used for the retrieval procedures, the LHMs were shown to be characterized by the effective parameters of permittivity (ε_{eff}) and permeability (μ_{eff}), and even refractive index (n_{eff}) and impedance (Z_{eff}).

In this study, we present the experimental measurements on one-dimensional (1D) and two-dimensional (2D) LHMs. Finite difference time domain (FDTD) simulations were performed to compare the experimental results. Effective permeability and permittivity values were retrieved from the simulated transmission and reflection coefficients. Impedance was shown to be matched to the free-space impedance at a narrow frequency region, which also corresponds to the frequency of the dip in the reflection spectrum.

2. REFLECTION FROM 1D LHM

The common design to construct a LHM is to arrange SRRs and wires in a periodic manner. The LHM samples that were used in the reflection measurements are obtained by patterning SRRs on the front side and the continuous wires on the other side of the dielectric board. A schematic picture of such a composite LHM is given in Figure 1(a). The darker patterns belong to the thin metal sheet and the lighter patterns belong to the dielectric board. The dielectric board is an FR4 printed circuit board (PCB) and the deposited metal is copper. The geometrical parameters of the SRR and wire can be found in a previous work [5].

The experimental measurement setup for measuring the reflection coefficient consists of a HP 8510C network analyzer and standard high-gain microwave horn antennas. The incident EM wave propagates along the x direction, while $\mathbf{E}$ is along the y direction, and $\mathbf{H}$ is along the z direction [see Fig. 1(a) for the directions]. Transmitter and receiver horn antennas were placed close to each other by keeping the angle between the antennas very small. The schematic picture depicting the top view of the experimental setup is given in Figure 1(c). The transmitter horn antenna sends the EM wave to the first surface of the structures and the receiver antenna measures the amplitude of the reflected EM waves. For calibration purposes, we placed a thick (~2 cm) slab of metal at a distance of 12 cm away from the antennas. Since metals reflect all of the incident EM waves at microwave frequencies, the reflection data from the metal can be set as the calibration data. The structures were then placed at the same distance from the antennas and the reflection coefficient was measured. It is worth mentioning at this point that the reflection measurements were all performed in free space rather than a waveguide environment. Therefore, we measure the reflections only from the surface of the LHM.

LHM is periodic along the x and y directions with a lattice constant of $a_x = a_y = 8.8$ mm. The periodicity along the z direction is achieved by stacking planar SRR planes with a lattice constant of $a_z = 6.5$ mm. The number of unit cells along the x, y, and z directions are $N_x = 5$, $N_y = 20$, and $N_z = 25$. The structure could respond to the EM wave only in one direction; therefore, the LHM is considered to be 1D. The measured and calculated reflection spectra of 1D LHM are provided in Figure 2. This structure was previously shown to exhibit true left-handed behavior with a transmission band between 3.55 and 4.05 GHz [5]. The effective permittivity and permeability were both negative at these frequencies. As clearly seen in Figure 2, both the experimental data and numerical simulations show a sharp dip in the reflection spectra of 1D LHM. The dip in the reflection spectrum is measured at 3.75 GHz with a dip value of −39.9 dB. FDTD simulations were performed to check the experimental results. The simulation results also calculated a similar dip in the reflection. In this case, the dip is located at 3.72 GHz and the reflection at this frequency is −40.2 dB. The agreement between the experimental results and theoretical calculations is quite good.

We also performed reflection measurements on a composite metamaterial (CMM), where the SRR structure was replaced with two concentric rings without splits [Fig. 1(b)]. The splits in the SRR structure play a key role for obtaining magnetic resonance. Removing the splits will prevent current from flowing between the inner and outer rings. Since there is no more current flowing between the concentric rings, the magnetic resonance will be destroyed [5, 26]. The resulting structure is called a closed ring

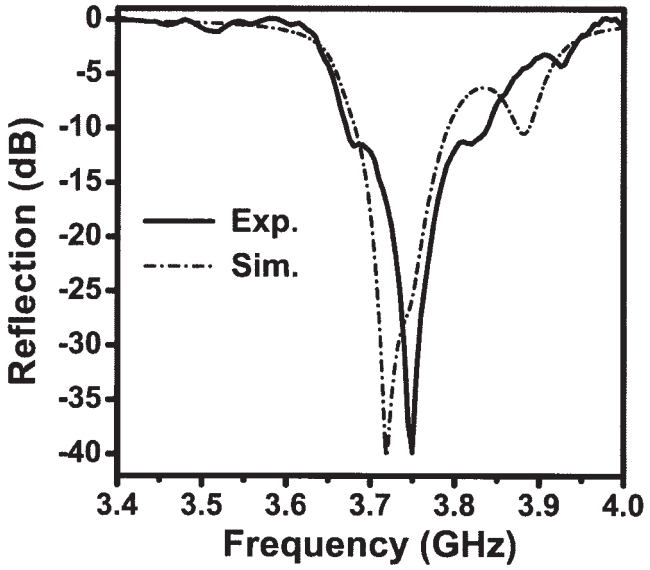

Figure 2 Reflection spectra of a 5-layer 1D LHM structure obtained via experimental measurement (solid) and FDTD simulations (dashed-dotted)

resonator (CRR) as a convention. The transmission spectrum of CMM composed of CRR and thin wire arrays can be found in previous work [5]. The left-handed transmission band is no longer present for the CMM case, because the magnetic permeability is positive because of lack of magnetic resonance. The measured reflection spectrum of CMM is shown in Figure 3 with a dashed-dotted line. The CMM structure reflects most of the incident EM waves throughout the frequency spectrum. However, the EM waves incident to the LHM structure around 3.75 GHz are nearly transmitted through the LHM without being reflected at the surface. This measurement indicates that the negative permeability of SRRs is responsible for the dip in the reflection spectrum of LHMs.

3. IMPEDANCE MATCHING

Before we commence retrieving the effective parameters of the LHM, we need to recall the reflection coefficient of an EM wave for the electric field perpendicular to the plane of incidence case [27]:

$$r = \frac{\sqrt{\frac{\varepsilon_0}{\mu_0}}\cos\theta_i - \sqrt{\frac{\varepsilon_1}{\mu_1}}\sqrt{1-\left(\frac{n_0}{n_1}\right)^2\sin^2\theta_i}}{\sqrt{\frac{\varepsilon_0}{\mu_0}}\cos\theta_i + \sqrt{\frac{\varepsilon_1}{\mu_1}}\sqrt{1-\left(\frac{n_0}{n_1}\right)^2\sin^2\theta_i}}. \quad (1)$$

In the above formula, the EM wave is assumed to be incident from the air to the LHM surface with an incident angle of θ_i. The refractive index is given by $n = \sqrt{\varepsilon\mu}$ and the impedance of the medium is $Z = \sqrt{\mu/\varepsilon}$. For free space, $\varepsilon_0 = \mu_0 = 1$ and therefore $n_0 = 1$ and $Z_0 = 1$. For $\theta_i = 0$, the EM waves are normally incident to the LHM surface. Equation (1) is reduced to:

$$r = \frac{Z_1 - Z_0}{Z_1 + Z_0}, \quad (2)$$

where Z_1 is the impedance of the LHM and Z_0 is the free-space impedance. It is obvious from Eq. (2) that if the impedance of the LHM is matched to free space, the reflection coefficient will be zero. Naturally occurring materials are not matched to free space. However, LHM has an advantage in achieving impedance matching, since their effective permeability and permittivity are strongly frequency dispersive. One can control the permeability and permittivity of the LHM layer, and impedance matching can therefore be obtained.

Since the impedance is defined as $Z = \sqrt{\mu/\varepsilon}$, one expects to have an impedance-matched medium for the case where the real parts of the effective permittivity and the permeability are equal ($\varepsilon_{\text{eff}} = \mu_{\text{eff}}$). We have employed the retrieval procedure to obtain effective parameters Z_{eff}, ε_{eff}, and μ_{eff}. We followed the approach outlined in Ref. [21]. The advantage of this procedure is that the correct branch of the effective refractive index and effective impedance was selected. The ambiguity in the determination of the correct branch is resolved by using an analytic continuation procedure. In the retrieval procedure, we employed a single layer of LHM along the propagation direction [x axis in Fig. 1(a)]. The periodic boundary conditions were set along the other directions (y and z axes). Hence, the simulation setup coincides with a slab of LHM that consists of single layer. The effective permittivity and permeability values were then derived from the transmission and reflection coefficients of the single layer of LHM.

Figure 4 displays the real parts of, ε, μ, and Z. Dielectric permittivity is negative below the plasma frequency $f = 8$ GHz [5]. Effective magnetic permeability of LHM is strongly dispersive around the magnetic resonance frequency, and approaches $\mu = 1$ for the lower and upper frequency limits. At the frequency $f = 3.71$ GHz, the real parts of permittivity and permeability are equal, $\varepsilon = \mu = -2.92$. Therefore, at this specific frequency, the condition $Z_0 = Z_1 = 1$ is satisfied. The simulated reflection spectrum exhibits a dip at 3.72 GHz. Therefore, the ultralow reflection observed in experiments and theoretical calculations is due to the impedance matching of LHM to free space.

Matching the impedance of LHM to free-space impedance is an important advance, since such a behavior is required for obtaining a perfect lens. Perfect lens was proposed by Pendry, which restores not only the phase of propagating waves but also the amplitude of evanescent modes by virtue of a negative refractive index [11]. The condition for satisfying such a perfect imaging mechanism is

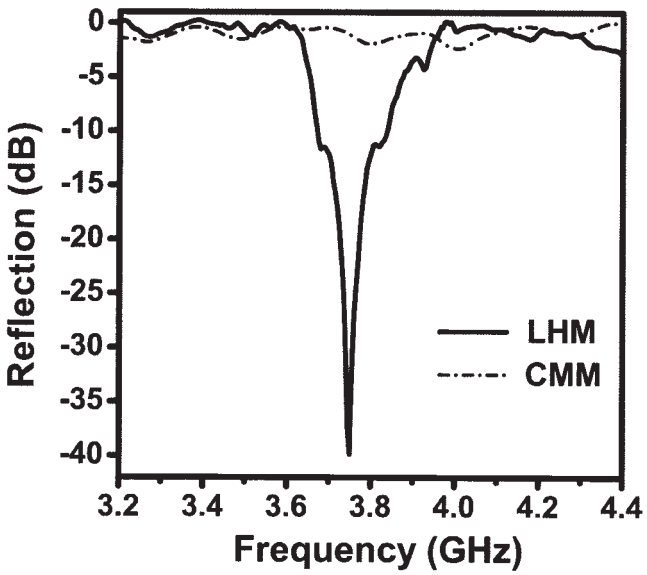

Figure 3 Measured reflection spectra of 5-layer 1D LHM (solid) and CMM (dashed-dotted) structures

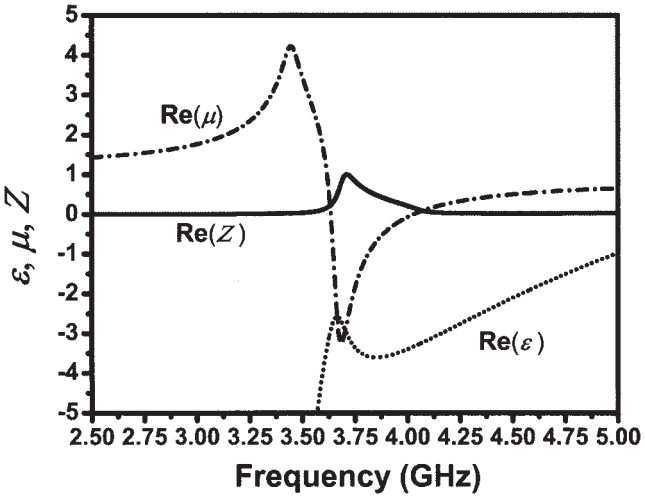

Figure 4 Real parts of effective permittivity, permeability, and impedance of LHM obtained by theoretical calculations using retrieval procedure

to use a material with $\varepsilon = \mu = -1$. Then, the refractive index will be $n = -1$ and the impedance is perfectly matched to free space, since $Z = 1$. It is proven that the sign of refractive index is negative, and the impedance is positive for negative permittivity and permeability values [16].

The first interface of such a perfect lens shows no reflection. Additionally, at the second interface, EM waves are perfectly transmitted into free space. It is easily deducible from Eq. (1) that such a structure is perfectly matched to free space for all angles of incidences. Optical properties of an impedance matched medium for $n = -1$ and $n \neq -1$ were investigated by means of theoretical calculations [28].

The LHM structure proposed here is impedance matched to the air only for the normal incidence of EM waves. As seen in Eq. (1), the angular part will contribute to the reflection coefficient for the angles of incidence $\theta_I \neq 0$, since the refractive index of LHM is $n \neq -1$. The reflection may be minimized by matching the impedance, provided that the values of the refractive indices are similar.

The impedance-matched frequency range is narrow as seen in Figure 2. It is expected to have a narrow frequency range for matched impedance, since μ_{eff} of SRRs is known to vary rapidly between the magnetic resonance (ω_{mo}) and magnetic plasma frequencies (ω_{mp}), although ε_{eff} of wires varies slowly throughout the frequency spectrum.

Although the reflection spectra of SRR-only and wire-only media were studied previously [29, 30], to our knowledge, no experimental evidence of impedance matched LHM exists. Impedance matching at the surface of a metamaterial is desirable, since it reduces the complications of the front face reflections, and assures that the negatively refracted beam is not the result of any experimental artifacts. Therefore, much more energy will be transferred inside the LHM at the impedance-matched frequencies. Moreover, the losses due to the reflection will be minimized and higher transmission values can be obtained.

4. REFLECTION FROM 2D LHM

In this section, we investigate the reflection characteristics of a 2D LHM structure. 2D LHM is constructed by stacking SRR planes along the x and z directions with lattice spacings of $a_x = a_z = 9.3$ mm. The periodicity of SRRs along the y direction is $a_z = 9.3$ mm, whereas the wires are continuous along the y axis [7, 8]. The number of unit cells is along the y and z axes and are $N_y = 20$ and

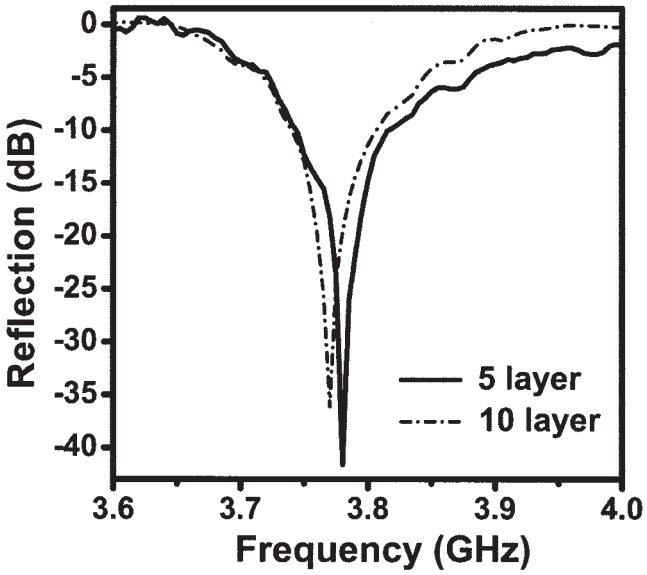

Figure 5 Measured reflection spectra of 2D LHM structures with a number of layers along the propagation direction (x) $N_x = 5$ (solid) and $N_x = 10$ (dashed-dotted)

$N_z = 40$. We have employed 2D LHM samples with two different numbers of layers along the propagation direction of EM waves. Reflection spectra of these two different numbers of layers are plotted in Figure 5. The dip at the reflection spectrum of LHM with $N_x = 5$ layers (solid line) was measured to be at 3.78 GHZ with a dip value of -41.6 dB. For $N_x = 10$ layers (dashed-dotted line), the dip is observed with a value of -36.1 dB at 3.77 GHz. Similar to the 1D LHM structure, 2D LHM reflects nearly all of the incident EM waves for a narrow frequency region. As clearly seen in Figure 5, the frequency did not change considerably although the structure's thickness was doubled. Therefore, this low reflection frequency regime cannot be due to the thickness resonance or Fabry-Perot resonance. The EM waves are mainly reflected from

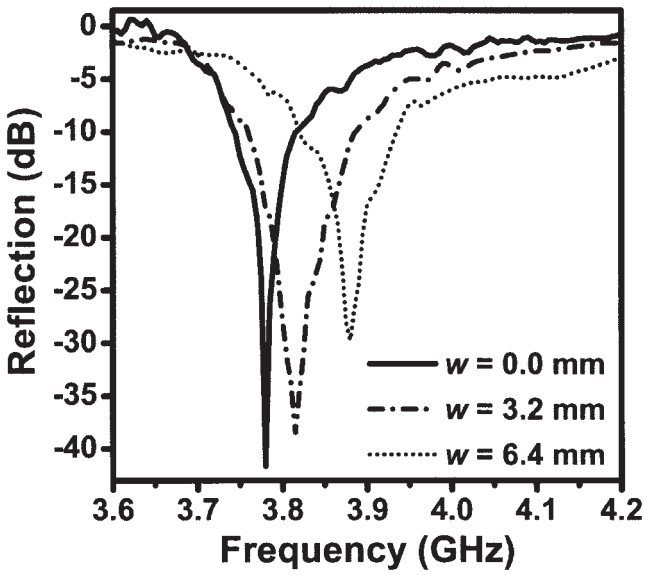

Figure 6 Measured reflection spectra of 2D LHM structures with dielectric boards of thicknesses $w = 0.0$ mm (solid), $w = 3.2$ mm (dashed-dotted), and $w = 6.4$ mm (dotted) placed to the air–LHM interface

the first surface of LHMs; changing the size of LHM would not affect the impedance-matched frequency.

Since the reflection is mainly from the first surface of LHM, we investigated the effect of inserting dielectric material at the air–LHM interface on the reflection properties. We placed dielectric material with two different thicknesses and observed the change in the reflection spectra. Figure 6 plots the measured reflection spectra of LHM with dielectric boards of thicknesses $w = 3.2$ mm (dashed-dotted) and $w = 6.4$ mm (dotted) placed in front of LHM structure. Therefore, we corrugated the surface and the EM waves faced the dielectric boards before reaching the LHM surface. The frequency where the reflection dip was observed in turn shifted to higher frequencies along with the increased thickness of dielectric board. For the thickness $w = 3.2$ mm, the minimum reflection was measured as -38.5 dB at the 3.82 GHz, whereas for the $w = 6.4$ mm case, the frequency of the lowest reflection value (-29.7 dB) was observed at 3.88 GHz. These measurements clearly indicate that the impedance-matched frequency may be tuned by placing dielectric materials and subsequently corrugating the LHM–air interface.

5. CONCLUSION

In summary, we investigated the reflection characteristics of 1D and 2D LHM structures experimentally in free space. We observed a very sharp dip in the reflection spectra for both structures. The reflection was very low at 3.75 GHz with a dip value of -39.9 dB for 1D LHM, whereas for 2D LHM, the minimum reflection was -41.6 dB at 3.78 GHz. FDTD simulations were performed to obtain the reflection coefficient of 1D LHM. The numerical simulations are in good agreement with the experimental data. Effective parameters of the LHM structure were retrieved by using the retrieval procedure. Permittivity and permeability were both negative and equal at 3.71 GHz, implying that the impedance was matched to free space. We have confirmed that the frequency of the reflection dip did not change considerably with the change of number of unit cells along the propagation direction. Hence, this characteristic cannot be attributed to thickness resonance. The observed low reflection is due to the impedance matching between the air and LHM interface. This is an important advancement in metamaterial development, as when ε and μ are both equal and negative, a well-matched, negative index material is obtained.

ACKNOWLEDGMENTS

This work is supported by the European Union under the projects EU-DALHM, EU-NOE-METAMORPHOSE, EU-NOE-PHOREMOST, and TUBITAK under Project No. 104E090. One of the authors (E. Ozbay) also acknowledges partial support from the Turkish Academy of Sciences.

REFERENCES

1. V.G. Veselago, The electrodynamics of substances with simultaneously negative values of permittivity and permeability, Sov Phys Usp 10 (1968), 509–514.
2. J.B. Pendry, A.J. Holden, W.J. Stewart, and I. Youngs, Extremely low frequency plasmons in metallic mesostructures, Phys Rev Lett 76 (1996), 4773–4776.
3. J.B. Pendry, A.J. Holden, D.J. Robbins, and W.J. Stewart, Magnetism from conductors and enhanced nonlinear phenomena, IEEE Trans Microw Theory Tech 47 (1999), 2075–2084.
4. D.R. Smith, W.J. Padilla, D.C. Vier, S.C. Nemat-Nasser, and S. Schultz, Composite medium with simultaneously negative permeability and permittivity, Phys Rev Lett 84 (2000), 4184–4187.
5. K. Aydin, K. Guven, M. Kafesaki, L. Zhang, C.M. Soukoulis, and E. Ozbay, Experimental observation of true left-handed transmission peak in metamaterials, Opt Lett 29 (2004), 2623–2625.
6. R.A. Shelby, D.R. Smith, and S. Schultz, Experimental verification of a negative index of refraction, Science 292 (2001), 77–79.
7. K. Aydin, K. Guven, C.M. Soukoulis, and E. Ozbay, Observation of negative refraction and negative phase velocity in left-handed metamaterials, Appl Phys Lett 86 (2005), 124102.
8. K. Aydin and E. Ozbay, Negative refraction through an impedance-matched left-handed metamaterial slab, J Opt Soc Am B 23 (2006), 415–418.
9. S.A. Cummer and B. Popa, Wave fields measured inside a negative refractive index metamaterial, Appl Phys Lett 85 (2004), 4564–4566.
10. I.V. Lindell, S.A. Tretyakov, K.I. Nikoskinen, and S. Ilvonen, BW media–media with negative parameters, capable of supporting backward waves, Microw Opt Technol Lett 31 (2001), 129–133.
11. J.B. Pendry, Negative refraction makes a perfect lens, Phys Rev Lett 85 (2000), 3966–3969.
12. K. Aydin, I. Bulu, and E. Ozbay, Focusing of electromagnetic waves by a left-handed metamaterial flat lens, Opt Exp 13 (2005), 8753–8759.
13. T.J. Yen, W.J. Padilla, N. Fang, D.C. Vier, D.R. Smith, J.B. Pendry, D.N. Basov, and X. Zhang, Terahertz magnetic response from artificial materials, Science 303 (2004),1494–1496.
14. S. Linden, C. Enkrich, M. Wegener, J. Zhou, T. Koschny, and C. Soukoulis, Magnetic response of metamaterials at 100 terahertz, Science 306 (2004), 1351–1353.
15. V.M. Shalaev, W. Cai, U. Chettiar, H.-K. Yuan, A.K. Sarychev, V.P. Drachev, and A.V. Kildishev, Negative index of refraction in optical metamaterials, Opt Lett 30 (2005), 3356–3358.
16. R.W. Ziolkowski and E. Heyman, Wave propagation in media having negative permittivity and permeability, Phys Rev E 64 (2001), 1–15, 056625.
17. D.R. Fredkin and A. Ron, Effectively left-handed (negative index) composite material, Appl Phys Lett 81 (2002), 1753–1755.
18. T. Koschny, M. Kafesaki, E.N. Economou, and C.M. Soukoulis, Effective medium theory of left-handed materials, Phys Rev Lett 93 (2004), 1–4, 107402.
19. D.R. Smith, S. Schultz, P. Markos, and C.M. Soukoulis, Determination of effective permittivity and permeability of metamaterials from reflection and transmission coefficients, Phys Rev B 65 (2002), 1–5, 195104.
20. T. Koschny, P. Markos, D.R. Smith, and C.M. Soukoulis, Resonant and anti-resonant frequency dependence of the effective parameters of metamaterials, Phys Rev E 68, (2003), 1–4, 065602(R).
21. X. Chen, T.M. Grzegorczyk, B. Wu, J. Pacheco, Jr., and J.A. Kong, Robust method to retrieve the constitutive effective parameters of metamaterials, Phys Rev E 70 (2004), 1–7, 016608.
22. X. Chen, B. Wu, J.A. Kong, and T.M. Grzegorczyk, Retrieval of the effective constitutive parameters of bianisotropic metamaterials, Phys Rev E 71 (2005), 1–9, 046610.
23. D.R. Smith, D.C. Vier, Th. Koschny, and C.M. Soukoulis, Electromagnetic parameter retrieval from inhomogeneous metamaterials, Phys Rev E 71 (2005), 1–11, 036617.
24. B. Popa and S.A. Cummer, Determining the effective electromagnetic properties of negative-refractive-index metamaterials from internal fields, Phys Rev B 72 (2005), 1–5, 165102.
25. D. Seetharamdoo, R. Sauleau, K. Mahdjoubi, and A.-C. Tarot, Effective parameters of resonant negative refractive index metamaterials, J Appl Phys 98 (2005), 1–4, 063605.
26. K. Aydin, I. Bulu, K. Guven, M. Kafesaki, C.M. Soukoulis, and E. Ozbay, Investigation of magnetic resonances for different split-ring resonator parameters and designs, New J Phys 7 (2005), 168.
27. J.D. Jackson, Classical electrodynamics, Wiley, New York, 1998, p. 305.
28. P.F. Loschialpo, D.W. Forester, D.L. Smith, F.J. Rachford, and C. Monzon, Optical properties of an ideal homogeneous casual left-handed metamaterial slab, Phys Rev E 70 (2004), 1–11, 036605.
29. E. Ozbay, K. Aydin, E. Cubukcu, and M. Bayindir, Transmission and reflection properties of composite double negative metamaterials in free space, IEEE Trans Antennas Propag 51 (2003), 2592–2595.
30. R.W. Ziolkowski, Design, fabrication and testing of double negative metamaterials, IEEE Trans Antennas Propag 51 (2003), 1516–1529.